JOURNAL OF AGRICULTURAL AND FOOD CHEMISTRY

Article

pubs.acs.org/JAFC

Structural Profiling and Quantitation of Glycosyl Inositol Phosphoceramides in Plants with Fourier Transform Mass Spectrometry

Nina Blaas and Hans-Ulrich Humpf*

Institute of Food Chemistry, Westfälische Wilhelms-Universität Münster, Münster, Germany

Supporting Information

ABSTRACT: Glycosyl inositol phosphoceramides (GIPC) are the main sphingolipids in plants, and optimization of their extraction and detection is still in the focus of research. Mass spectrometry provides new options for the analysis and structural elucidation of this complex class of lipids. The coupling of linear ion trap and orbitrap (LTQ Orbitrap) enabled various fragmentation experiments (MS^2, MS^3) by collision-induced dissociation (CID) and pulsed-Q dissociation (PQD). For structural analysis, GIPC-fragment ions were detected in the positive and negative ion mode with exact masses; therefore, fragmentation patterns were observed and finally structures have been characterized regarding polar head group, fatty acid, and sphingoid base. GIPC profiling was performed for spinach, white cabbage, sunflower seeds, and soybeans. The total GIPC concentration in these plants ranged from 1.1 to 88.4 μg/100 g dry weight with t18:1/h24:0 as the main ceramide structure and hexose-hexuronic acid-inositol phosphate and *N*-acetylhexosamine-hexuronic acid-inositol phosphate as polar head groups.

KEYWORDS: *sphingolipids, GIPC, HPLC-MS/MS, FTMS, inositol, structure elucidation, Fourier transform mass spectrometry*

INTRODUCTION

Sphingolipids such as ceramides and cerebrosides have been analyzed in detail in plants due to the good solubility in organic solvents.[1] Because of their complex and polar structure not so much is known about glycosyl inositol phosphoceramides (GIPC). For this reason, we focused on this class of lipids in plants and developed an extraction and detection method using a mass spectrometric approach. GIPC were described for the first time by Carter, who characterized this lipid class in plant seeds.[2] Years later GIPC were also been identified in plants and fungi.[3−5] Similar glycosyl inositol phosphate groups are part of glycosylphosphatidylinositol (GPI)-anchor proteins.[6−8] Besides cerebrosides, GIPC are the major sphingolipids in plant cell membranes.[9] The structural diversity is based on the high variability of the structural elements: The nonpolar ceramide is formed by a long chain base with an amide-linked fatty acid, and the polar head group (saccharide chain) is attached via a phosphate group (Figure 1). Due to the amphiphilic character of GIPC, the extraction needs special attention.[10]

Markham et al. have identified the sphingoid bases t18:1 (8*Z* and 8*E*), t18:0, d18:2 (4*E*/8*Z* and 4*E*/8*E*), d18:1 (8*Z* and 8*E*), and d18:0 in GIPC in plants (nomenclature: d: dihydroxylated, t: trihydroxylated, the following numbers indicate the carbon atoms and double bonds). The sphingoid base-profile depends on the plant; however, the major base in the leaves of tomato, *Arabidopsis thaliana*, and soy is t18:1 (8*E*).[10] The grade of unsaturation of the sphingoid bases depends on the type of desaturase, as Δ4- or Δ8-sphingolipid desaturases have been identified.[10,11] The bound fatty acids have a chain length of C16−C26 atoms and are usually monohydroxylated in the α position.

The polar head group consists of different hexoses and pentoses such as glucose, galactose, glucuronic acid, glucosamine, *N*-acetylglucosamine, and arabinose.[12] Figure 1 shows a summary of the structural features of GIPC.

GIPC have been analyzed in the past by different mass spectrometric techniques. Quantitation was performed by high performance liquid chromatography coupled to tandem mass spectrometry (HPLC-MS/MS) using multiple reaction monitoring (MRM) mode;[11] by use of GM_1 ganglioside as internal standard, the GIPC concentration in *A. thaliana* was determined to be 236 nmol/g dry weight. IPC in fungi were analyzed by quadrupole time-of-flight (qTOF) and linear ion trap-orbitrap (LTQ Orbitrap).[13] Another successful GIPC screening in plants was performed by matrix-assisted laser desorption/ionization (MALDI) MS/MS.[14]

A combination of the above-mentioned methods together with the hydrolysis of intact GIPC followed by derivatization of the sphingoid bases and their analysis by gas chromatography is often performed for structural profiling. The aim of this project was the structural elucidation, profiling, and quantitation of GIPC by the use of a linear ion trap−orbitrap (LTQ Orbitrap) mass spectrometer. Plant material was extracted, and the GIPC structures were characterized by fragmentation experiments with collision-induced dissociation (CID) and pulsed-Q dissociation (PQD). So far, GIPC occurrence in spinach, white cabbage, sunflower seeds, and soybeans has not been determined. Structure elucidation of fatty acids, sphingoid bases, and polar head groups was performed based on detected and calculated exact masses of fragment ions in MS^2- and MS^3-experiments. As GIPC are not available as internal standards, quantitation was

Received: January 11, 2013
Revised: April 10, 2013
Accepted: April 10, 2013
Published: April 10, 2013

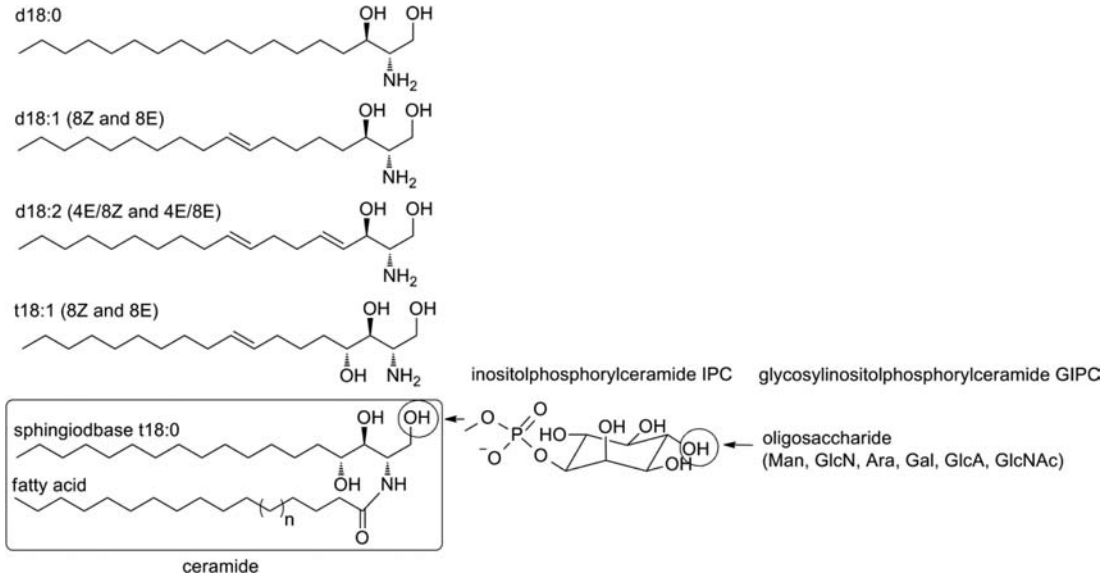

Figure 1. Basic structure of GIPC. Mentioned sphingoid bases were detected in GIPC of plants. Sugar derivatives such as mannose, glucosamine, arabinose, galactose, glucuronic acid, and *N*-acetylglucosamine belong to the polar head groups in various compositions.[10]

performed with the use of sphingosyl phosphoinositol (lyso-IPC) as internal standard and C17-inositol phosphoceramide (C17-IPC) as ionization standard.

MATERIALS AND METHODS

Material. Deep frozen spinach, fresh white cabbage, sunflower seeds, and dried soybeans were purchased at a local supermarket. *A. thaliana* plants were cultivated in collaboration with Prof. J. Kudla (University of Münster, Germany), and the leaves of tomato plants were collected from regional farmers.

Sphingolipid ceramide *N*-deacylase (SCDase) was purchased from Takara Bio. Inc. (Otsu, Japan). The magnetic macroporous cellulose beads (100 to 250 μm) were kindly provided by Dr. J. Lenfeld (Institute of Macromolecular Chemistry, Academy of Sciences of the Czech Republic, Prague, Czech Republic). All chemicals were of HPLC grade and purchased from Sigma-Aldrich GmbH (Seelze, Germany), Carl-Roth GmbH + Co. KG (Karlsruhe, Germany) or VWR International GmbH (Darmstadt, Germany). Water for HPLC separation and dialysis was purified by a Milli-Q Gradient A 10 system (Millipore, Schwalbach, Germany). Sphingosyl phosphoinositol (lyso-IPC) was purchased from Avanti Polar Lipids Inc. (Alabaster, AL)

Sample Preparation. The leaves were lyophilized, ground, and stored at −20 °C. The seeds and beans were ground after mixing with liquid nitrogen. The GIPC extraction method was described by Toledo et al. for fungal material.[15] The extraction solvent contained 2-propanol, *n*-hexane, and water in a ratio of 55:20:25 (v/v/v), and after complete separation, the upper phase was removed and discarded. A 20−30 g amount of the plant material was extracted with 400 mL of the extraction solvent for 1 h at room temperature on a shaker. After filtration under vacuum, the filtrate was again extracted with 2-propanol, *n*-hexane, and water and filtered. A third extraction of the filtrate was performed with 400 mL of chloroform/methanol (2:1, v/v) using an Ultra-Turrax at the highest adjustment for 5 min followed by 30 min on a shaker. The mixture was again filtered, and all filtrates were concentrated using a rotary evaporator with a water bath at 39 °C. Chlorophyll was precipitated by adding 400 mL of water to the residues; it was removed by filtration of the aqueous extracts of the leaves of spinach, tomato, *A. thaliana*, and white cabbage through a crude porous filter paper. After the removal of precipitated chlorophyll, the aqueous filtrate was concentrated by lyophilization and the residue stored at −20 °C. Plant material with a high content of lipids, such as sunflower seeds and dried soybeans, were defatted. A 50−75 g amount of ground material was mixed with 200 mL of *n*-hexane, the supernatant was removed, and new hexane was added. The sphingolipid extraction was performed with 200 mL of chloroform and methanol in a ratio of 2:1 (v/v) for 60 min, and after filtration, the extraction was repeated. The filtrates were combined and concentrated by rotary evaporation.

The enrichment of anionic compounds, such as phospholipids, was achieved by anion exchange chromatography. DEAE Sephadex A-25 (GE Healthcare, Uppsala, Sweden) was stored in chloroform, methanol, and water (30:60:8, v/v/v) before the first application. A glass column (i.d. 3 cm) was plugged by defatted cotton and filled up to 20 cm with DEAE material. The material was washed with 100 mL of chloroform/methanol/water (30:60:8, v/v/v). The freeze-dried plant extract was dissolved in chloroform/methanol/water (30:60:8, v/v/v) and loaded on the column. The first fraction was eluted with 300 mL of chloroform/methanol/water (30:60:8, v/v/v) for removal of neutral compounds, and the next fraction was eluted with 300 mL of methanol (second fraction). The elution of anionic compounds was obtained by methanolic NaOAc solution. For the third fraction, methanolic 0.3 M NaOAc was used, and the fourth fraction was eluted with 0.6 M NaOAc in methanol. The GIPC were part of the third fraction, and the fourth fraction was analyzed by HPLC-FTMS for residues of GIPC. The fractions were concentrated by rotary evaporation. Dialysis was performed for fractions three and four to remove NaOAc. The fractions were dissolved in 20−40 mL of Millipore water, and each was filled into a dialysis tube (Spectra/Por Dialysis Membrane, MWCO 3500, vol/length 9.3 mL/cm, Spectrum Laboratories. Inc., Rancho Dominguez, CA). The dialysis took place at 4 °C for three days, and the water was changed every 6 to 12 h. The desalted fractions were lyophilized and afterward dissolved in a volume of 1 to 5 mL of chloroform/methanol (2:1, v/v). This solution was stored at −20 °C. As glycerophospholipids would interfere during the mass spectrometric analysis of GIPC, they were removed by alkaline hydrolysis as described in the literature.[16] In this procedure, methanolic NaOH (1 M) was added to an aliquot of the stock solution to end up with a final NaOH concentration of 0.1 M. The hydrolysis took place at 37 °C for 3 h. After neutralization with HCl (1 M), the solution was dried under a stream of nitrogen and dissolved in a known volume of 1 to 5 mL of chloroform/methanol (2:1, v/v). For mass spectrometric analysis, an aliquot was concentrated and dissolved in tetrahydrofuran/methanol/water 0.1% formic acid (2:1:2, v/v/v), which is in accordance with the starting conditions of the HPLC gradient.

HPLC-FTMS Analysis for Structural Profiling and Quantitation. Mass spectrometric experiments were performed on an LTQ Orbitrap XL mass spectrometer (Thermo Fisher Scientific, Bremen, Germany) coupled to an Accela LC 60057-60010 system (Thermo

Fisher Scientific). Data acquisition was performed with Xcalibur 2.07 SP1 (Thermo Fisher Scientific). For chromatographic separation, a 150 × 2.1 mm i.d., 5 μm Ascentis RP-Amide (Supelco, Bellefonte, PA) with a Varian Polaris C_8 precolumn 2 × 4 mm (Varian, Palo Alto, CA) was used at a column temperature of 40 °C. The binary gradient consisted of solvent A methanol/tetrahydrofuran (60:40, v/v) (0.1% formic acid and 5 mM ammonium formate) and solvent B water (0.1% formic acid and 5 mM ammonium formate) as follows: isocratic step at 80% solvent A for 5 min, followed by a linear gradient to 100% solvent A in 18 min. After each run, the column was equilibrated at the starting conditions. The flow rate was 200 μL/min, and the injection volume was 10−20 μL. The ionization was performed with heated electrospray ionization (HESI) in the positive and negative mode, depending on the fragmentation experiments, e.g., collision-induced dissociation (CID) and pulsed-Q dissociation (PQD). Fragment ions were detected by FTMS or by linear ion trap mass spectrometry (ITMS), both detection modes can be operated in parallel to each other. Source conditions were as follows in the negative mode: spray voltage, 3 kV; vaporizer temperature, 250 °C; capillary temperature, 225 °C; sheath gas, 35 arbitrary units (arb); auxiliary gas, 10 arb; capillary voltage, 89 V; tube lens voltage, 61 V; sweep gas 0 arb. Source conditions in the positive mode: spray voltage, 3.5 kV; vaporizer temperature, 350 °C; capillary temperature, 225 °C; sheath gas, 50 arbitrary units (arb); auxiliary gas, 10 arb; capillary voltage, 47 V; tube lens voltage, 189 V; sweep gas 5 arb. The resolution was set to 30.000 and the isolation width to m/z 2. Table 1 shows a list of calculated exact masses of various GIPC species.

Table 1. Calculated Exact Masses of GIPC Molecular Ions $[M - H]^-$ with Monohydroxylated Fatty Acids (Chain Length C15−C27) and Sphingoid Bases t18:0 and t18:1 (Retention Times Are Listed for Both GIPC Classes)

		hexose-GIPC		*N*-acetyl-GIPC	
fatty acid	sphingoid base	ret time, min	$[M - H]^-$, m/z	ret time, min	$[M - H]^-$, m/z
h15:0	t18:1	5.0	1134.5827		
h16:0	t18:1	5.1	1148.5984	5.1	1189.6250
h16:0	t18:0	5.6	1150.6141	5.6	1191.6407
h19:0	t18:1			8.5	1231.6721
h20:0	t18:1	7.8	1204.6612	9.2	1245.6878
h21:0	t18:1	10.0	1218.6768		
h22:0	t18:1	9.2	1232.6925	8.7	1273.7191
h22:0	t18:0			9.7	1275.7348
h23:0	t18:1	9.9	1246.7082	9.8	1287.7348
h24:0	t18:1	10.6	1260.7239	10.4	1301.7505
h24:0	t18:0	11.1	1262.7396	10.7	1303.7662
h25:0	t18:1	11.2	1274.7396	10.9	1315.7662
h25:0	t18:0			11.6	1317.7819
h26:0	t18:1			11.7	1329.7819
h26:0	t18:0	12.2	1290.7710	12.1	1331.7976
h27:0	t18:1	12.5	1302.7710		

Fragmentation Experiments by HPLC-FTMS^n and -ITMS^n. Method 1 for HPLC-CID-FTMS^2 and -ITMS^2 (Positive Ion Mode). The first scan event was a total ion scan ranging from m/z 1140 to m/z 1370. The relative fragmentation energy of CID was 35%. MS^2-spectra were monitored for all detectable ions, and their fragmentation patterns were compared. The results are shown in Figure 6 and Figure 9.

Method 2 for HPLC-CID-FTMS^2 and HPLC-PQD-ITMS^2 (Negative Ion Mode). The first scan event was a total ion scan ranging from m/z 1100 to m/z 1370. The relative fragmentation energy of CID and PQD was 35%. MS^2-spectra were monitored for all detectable ions, and their fragmentation patterns were compared. The parameters for the GIPC quantitation were slightly different: mass range from m/z 500−1500 with an isolation width of m/z 1.5. The results are demonstrated in Figures 2, 3, 5, and 9 and in Figures S1 and S2 (see Supporting Information).

Method 3 for Structural Analysis of the Ceramide Part by HPLC-MS^3 (Positive Ion Mode). The mass range was from m/z 180 to 1290. The relative fragmentation energy of CID-FTMS^2, CID-FTMS^3, CID-ITMS^2, and CID-ITMS^3 was 35% with an isolation width of m/z 2. The accurate mass of the GIPC molecular ion $[M + H]^+$ was detected, and in the second step the ceramide fragment ion $[Z_0 + H]^+$ was again fragmented to explore the MS^3-spectrum. The molecular ion and the ceramide fragment ion are presented in Figure 6. The following fragmentation experiments were performed: $[M + H]^+$ to $[Z_0 + H]^+$; 1234.7082 to 636.5910; 1236.7239 to 638.6067; 1262.7396 to 664.6220; 1264.7553 to 666.6367; 1290.7710 to 692.6523; 1276.7553 to 678.6377; 1304.7867 to 706.6690 (see Figure 7).

Method 4 for Structural Analysis of the Polar Head Group by HPLC-MS^3 (Negative Ion Mode). The mass range was from m/z 250 to 1330. The relative fragmentation energy of CID-FTMS^2 was 35−40%, CID-FTMS^3 35%, PQD-ITMS^2 35%, and PQD-ITMS^3 40% with an isolation width of m/z 2. The accurate mass of the GIPC molecular ion $[M - H]^-$ was detected, and in the second step the polar head group fragment ion $[C_3PO_3 - H]^-$ was again fragmented to explore the MS^3-spectrum. For example $[M - H]^-$ to $[C_3PO_3 - H]^-$: 1301.7505 to 638.1324; 1278.7348 to 638.1324; 1258.7082 to 597.1060; 1260.7239 to 597.1060; 1232.6925 to 597.1060 (see Figure 8).

Synthesis of C17-Inositol Phosphoceramide (C17-IPC). Immobilization of SCDase on Magnetic Macroporouse Cellulose Beads. The procedure was described by Kuchar et al.[17] and is briefly summarized here. The particles were stored in a small volume of PBS-buffer (pH 7.0) to cover the material with liquid. A 100 μL amount of the particle-buffer solution was transferred to a 4 mL screw-cap vial and combined with aqueous $NaIO_4$ solution (0.2 M, 100 μL). After the vial was shaken for 90 min at room temperature, the particles were washed 10 times with PBS-buffer (pH 7.0). The particles were suspended in 100 μL of PBS-buffer, and 62.5 mU (12.5 μL) of SCDase was added. After the mixture was shaken for 10 min at room temperature, $NaCNBH_3$ (3 mg/mL, 200 μL) was added to the reaction solution. The reaction was stirred overnight at 4 °C, and afterward the particles with immobilized SCDase were washed three times with 1 to 2 mL of PBS-buffer (pH 7.0), three times with PBS-buffer (1 M NaCl, pH 7.0), and finally with PBS-buffer (pH 7.0). The particles were stored in PBS-buffer 0.1% Triton-X (pH 7.0) at 4 °C.

Synthesis of C17-IPC by Immobilized SCDase. A 1.5 mL screw-cap vial was utilized as a reaction tube. A 37 nmol amount of heptadecanoic acid C17-FA (20 μL of a stock solution with 1 mg/mL in ethanol) and 25 nmol of lyso-IPC (13.5 μL of a stock solution with 1 mg/mL in tetrahydrofuran/methanol/water (2:1:2, v/v/v)) were combined and dried under a stream of nitrogen at 39 °C. The immobilized particles (25 μL) were added to the educts, and 200 μL of PBS-buffer (0.1% Triton-X, pH 7.0) was used as reaction solvent. The closed tube was slightly shaken and stored at 37 °C. The conversion was determined by analyzing aliquots after different time points via HPLC-MS/MS in the positive MRM-mode. As soon as the reaction was completed, the particles were fixed on the bottom by contact to a magnet. The supernatant could easily be collected, and the particles were washed several times to recover synthesized C17-IPC. The immobilized SCDase on magnetic macroporous cellulose beads was reused after washing with PBS-buffer.

The reaction mixture was collected and stored at −20 °C until cleanup. The supernatants were dried under a stream of nitrogen, dissolved in 50 μL of tetrahydrofuran/methanol/water 0.1% formic acid (2:1:2, v/v/v), filled into a vial-insert, and further purified using HPLC. The HPLC system was connected to a fraction collector (200 μL/minute), and the separation was carried out by an analytical RP-Amide column. A linear gradient started with 30% of solvent B (MeOH/THF (60:40, v/v) 0.1% formic acid) and 70% of solvent A (water 0.1% formic acid, 5 mM ammonium formate) for 1 min and then to 100% of solvent B over 15 min. All fractions were concentrated by a vacuum concentrator, and the remaining water was removed by lyophilization. The residue was dissolved in 1 mL of tetrahydrofuran/methanol (3:2, v/v). For mass spectrometric analysis, aliquots (10 μL) of all fractions were diluted with 40 μL of tetrahydrofuran/methanol/water 0.1% formic acid for a final concentration of C17-IPC equal to 1−2 nmol. The obtained

fractions were analyzed by HPLC-MS/MS in the positive MRM-mode, and fractions containing the desired product were combined and stored at −20 °C. Solid-phase extraction with Strata-X 33, a polymeric reversed phase material (200 mg/3 mL, Phenomenex, Aschaffenburg, Germany), was used as final cleanup step. Conditioning of the column was performed by eluting with different solvents as follows: 15 mL of chloroform, 15 mL of methanol, and 15 mL of water. C17-IPC was dissolved in 10 mL of water, loaded on the column, and washed with 10 mL of water to remove salts and polar compounds. The percentage of organic solvent was increased from 8 mL of methanol/water (1:1, v/v) in the beginning to 9 mL of methanol to finally elute the nonpolar C17-IPC. The fractions were collected in 1.5 mL vials. Chloroform (10 mL) was applied to prove that all of the C17-IPC had been eluted previously. The fractions were dried using a vacuum concentrator at 39 °C, and residues were dissolved in tetrahydrofuran/methanol (3:2, v/v) and analyzed by HPLC-FTMS. The fractions with C17-IPC were combined (yield: 2 mg). The fragmentation pattern (data not shown) of the $[M - H]^-$ of lyso-IPC with m/z 540.2943 and for C17-IPC with m/z 792.5396 showed the loss of inositol, detected by the mass difference of 162.0535−162.0567 u (exact mass of m/z 162.0528). The resulting sphingoid base-phosphate fragment ion had an m/z of 378.2408 (exact mass m/z 378.2415), and the ceramide-phosphate fragment ion had an m/z of 630.4829 (exact mass of m/z 630.4868). Both spectra showed the fragment ions of $[IP]^-$ with m/z 259.0222 and of $[IP - H_2O]^-$ with m/z 241.0117.

HPLC-MS/MS Parameters. The reaction conversion was proven by mass spectrometric experiments on an API 4000 QTrap mass spectrometer (ABI Sciex, Darmstadt, Germany) coupled to an Agilent 1100 series HPLC (Agilent Technologies, Waldbronn, Germany). Data acquisition was performed with Analyst 1.4.2 software (ABI Sciex, Darmstadt, Germany). For chromatographic separation, a 150 × 2.1 mm i.d., 5 μm Ascentis RP-Amide (Supelco, Bellefonte, PA) was used at a column temperature of 40 °C. The binary gradient consisted of solvent A methanol/tetrahydrofuran (60:40, v/v) (0.1% formic acid and 5 mM ammonium formate) and solvent B water (0.1% formic acid and 5 mM ammonium formate) as follows: isocratic step at 70% solvent A for 1 min, followed by a linear gradient to 100% solvent A in 14 min. After each run, the column was equilibrated at starting conditions. The flow rate was 200 μL/min, and the injection volume was 10 μL. The mass spectrometer was operated in the positive multiple reaction monitoring mode (+MRM). The resolution for Q1 and Q3 was set at ±0.35 amu. Nitrogen (4.5×10^{-5} Torr) served as collision gas. Zero-grade air was used as nebulizer gas (35 psi) and was heated at 350 °C, and as turbo gas for solvent drying (45 psi). The ion spray voltage was set at 5.5 kV, DP (declustering potential) at 101 V, CE (collision energy) at 30 V, and CXP (cell exit potential) at 18 V.

MRM transitions for lyso-IPC were m/z 542.3 to 282.2, m/z 542.3 to 264.2, and for C17-IPC were m/z 794.5 to 534.4, m/z 794.5 to 516.4. The retention time of lyso-IPC was 4.2 min and for C17-IPC was 14.8 min.

Analysis of the Purity of C17-IPC and Lyso-IPC. The purity was confirmed by HPLC with evaporative light scattering detection (HPLC-ELSD) with a LC-20AT system (Shimadzu Corporation, Kyoto, Japan). Data acquisition was performed with Shimadzu LCsolution Version 1.21 SP1. The parameters for the ELSD were as follows: nitrogen gas pressure of 2.5 bar and a temperature of 40 °C.

The binary gradient consisted of solvent A water (0.1% formic acid and 5 mM ammonium formate) and solvent B methanol/tetrahydrofuran (60:40, v/v) (0.1% formic acid): isocratic step at 70% solvent B for 1 min, followed by a linear gradient to 100% solvent B in 14 min; after 3 min, the gradient was changed to the starting conditions for equilibration of the column. The flow rate was 200 μL/min and the injection volume 10 μL. The GIPC amounts were corrected regarding the purity of the standard lyso-IPC (74% HPLC-ELSD). The purity of C17-IPC was 28% (HPLC-ELSD) whereas salts eluting in the dead volume of the column were the major impurities with 70%. HPLC-FTMS analysis (negative ion mode) resulted in a purity of 92%, as salts are not detectable.

Quantitation of GIPC. The quantitation was performed by HPLC-FTMS in the negative ion mode, using the parameters as described above (method 1). Commercially available lyso-IPC was applied as standard, and the following concentrations of 10, 25, 50, 100, 200, and 250 ng/mL in tetrahydrofuran/methanol/water 0.1% formic acid (2:1:2, v/v/v) were used for a calibration curve. In addition to lyso-IPC, the synthesized C17-IPC (stored in tetrahydrofuran/methanol (3:2, v/v)) was used as ionization standard. The extracts of the different plant materials and all samples of the calibration curve were spiked with the same amount of C17-IPC (final concentration 50 μg/mL). The use of C17-IPC minimized ionization effects due to coeluting matrix compounds. The plant extracts were analyzed in duplicate. To calculate the GIPC amount in the plant samples, the peak area ratios of lyso-IPC of the calibration curve and of the ionization standard C17-IPC were plotted against their concentration ratios. The GIPC content of hexose-hexuronic acid-inositol phosphoceramide and *N*-acetylhexosamine-hexuronic acid-inositol phosphoceramide are reported as μg GIPC per 100 g dry weight of sample (Figure 10, Figure 11, and Figure S3 in the Supporting Information).

RESULTS AND DISCUSSION

Extraction Procedure and Basic MS Experiments for the Isolation and Structure Elucidation of GIPC. Glycosyl inositol phosphoceramides (GIPC) were analyzed in different plant materials such as spinach, white cabbage, sunflower seeds, and soybeans. The leaves of tomato and *A. thaliana* were used as reference material, as GIPC content has already been characterized.[10] The extraction method, the chromatographic conditions for the separation by high performance liquid chromatography (HPLC), and the parameters for the mass spectrometric analysis by Fourier transform mass spectrometry (FTMS) were developed by using this reference material with a known profile of GIPC.

The extraction step is based on a liquid extraction with a mixture of 2-propanol/*n*-hexane/water (55:20:25, v/v/v), which was described by Markham et al. as the optimized GIPC extraction solvent system.[10] Due to the phosphate group, GIPC are anionic compounds, and sample cleanup and concentration were performed by anion-exchange chromatography with diethylaminoethyl (DEAE) material.[18] Glycerophospholipid content was removed by alkaline hydrolysis to avoid any mass spectrometric interferences.[16] For structure elucidation of GIPC species, detailed HPLC-FTMS experiments were performed. MS^2- and MS^3-spectra with high mass accuracy were performed by isolation and fragmentation of precursor ions in the linear ion trap. The spectra were acquired by using either the orbitrap for higher mass accuracy or the linear ion trap for better sensitivity. FTMS-detection enabled the determination of definite elemental compositions of detected molecular ions and of their fragment ions.[13]

Fragmentation experiments as $FTMS^2$ and $FTMS^3$ in the positive and negative ion mode were performed for structural investigations of the ceramide part and the polar head group. For structure elucidation, MS measurements in the positive and negative mode are possible, as the phosphate group stabilizes negative molecular ions $[M - H]^-$ and the amide-linkage positive molecular ions $[M + H]^+$. Single-charged GIPC were screened in the mass range of m/z 1100 to 1350 in the positive and negative ion mode. MS^2-spectra were generated by collision-induced dissociation (CID) and pulsed-Q dissociation (PQD). The mass range of CID-fragmentation spectra is limited for the used mass spectrometer by the molecular weight of the molecular ion, as the lowest m/z value of fragment ions is 25% of the m/z of the molecular ion. The MS^2-spectrum of a GIPC with a m/z of 1260 would result only in fragment ions above $m/z > 315$, which limits structural information. In contrast PQD-fragmentation

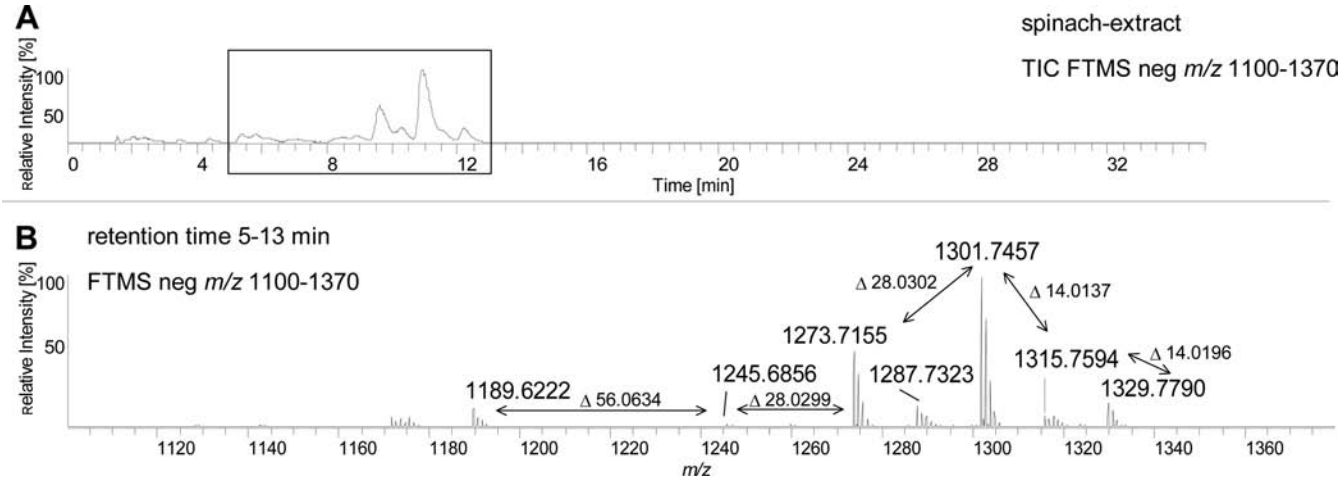

Figure 2. (A) HPLC-FTMS-TIC chromatogram of a spinach extract (mass range of m/z 1100−1370 in the negative ion mode). (B) FTMS-spectrum of molecular ions with a retention time of 5−13 min. The molecular ions possessed mass differences of Δ 14.0137−14.0196 u, Δ 28.0299−28.0302 u, and Δ 56.0634 u (HPLC-FTMS method 2).

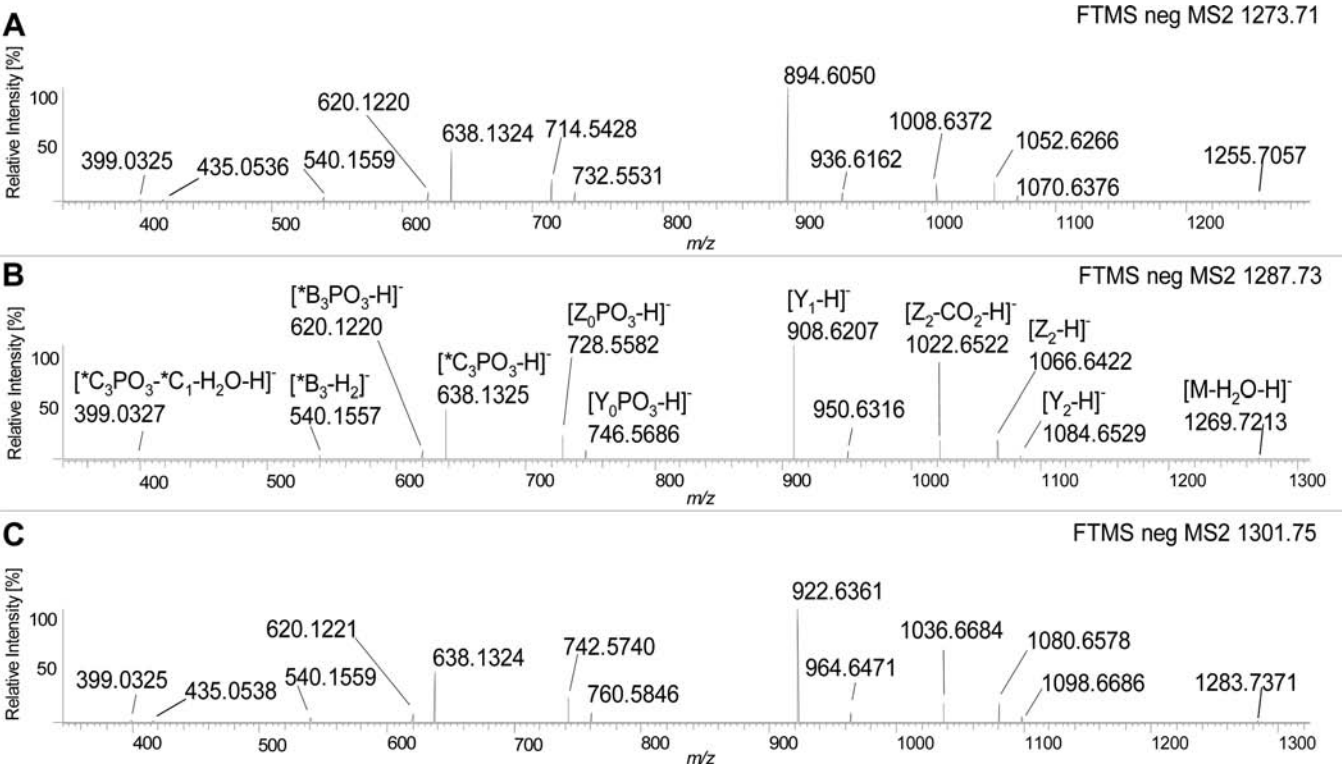

Figure 3. CID-FTMS^2-product ion spectra of $[M - H]^-$ m/z 1273.7155 (A), m/z 1287.7323 (B), and m/z 1301.7457 (C) in spinach. Fragment ions in the mass range of m/z 399−638 were identical in spectra A, B, and C. Fragment ions with m/z > 700 showed a difference of 14.01 u from spectra A to B and B to C (HPLC-FTMS method 2).

leads to the detection of fragment ions in the ion trap to m/z > 50 independent of the molecular weight.

Structure Elucidation of GIPC in Plant Species. *Structure Elucidation by FTMS in the Negative Ion Mode.* After the confirmation of known GIPC-species in leaves of *A. thaliana* and tomato, the extraction method and mass spectrometric approach was adapted to the plant samples spinach, white cabbage, sunflower seeds, and soybeans. Figure 2 shows a FTMS total ion chromatogram ranging from m/z 1100 to 1370 in the negative mode (Figure 2A) of a spinach extract. The MS-spectra of the molecular ions with a retention time of 5 to 13 min are given in Figure 2B. The highest signal intensities were detected for the molecular ions m/z 1273.7155 and m/z 1301.7457. Mass differences of the obtained negatively charged molecular ions $[M - H]^-$ were either Δ 14.0137 to 14.0196 u, Δ 28.0299 to 28.0302 u, or Δ 56.0634 u, indicating different chain length with one, two, or four additional methylene groups.

The extracted mass chromatograms of m/z 1273.7155, m/z 1287.7323, and m/z 1301.7457 (see Figure S1 in the Supporting Information) showed an increasing retention time with rising molecular weight of the molecular ions. The gradual elongation by one methylene group indicates the presence of odd- and even-numbered carbon chain length of the sphingoid base or fatty acid.

dx.doi.org/10.1021/jf4001499 | J. Agric. Food Chem. 2013, 61, 4257−4269

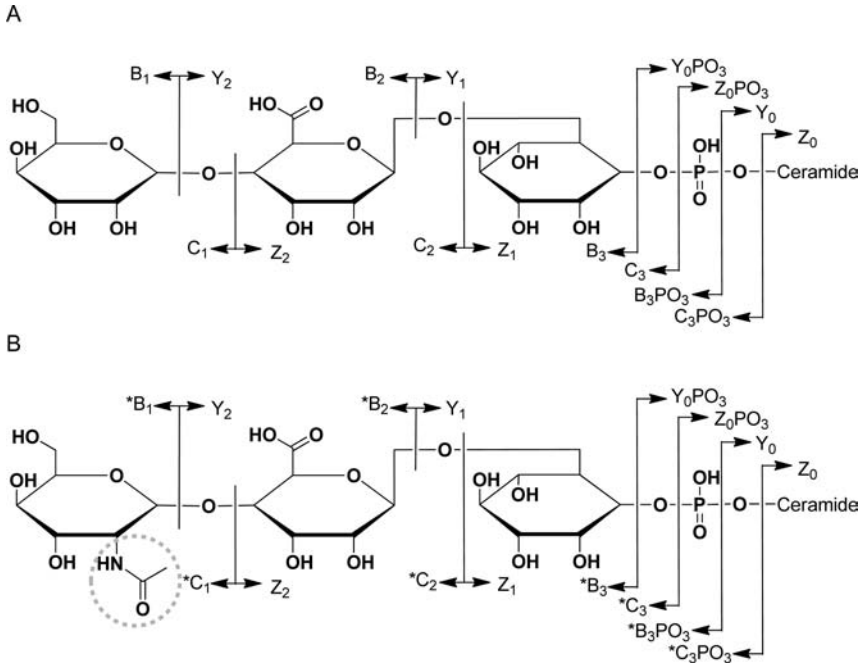

Figure 4. Nomenclature for characteristic fragment ions of GIPC species.[15,19] GIPC structures: (A) hexose-hexuronic acid-inositol phosphoceramide (hexose-GIPC) and (B) *N*-acetylhexosamine-hexuronic acid-inositol phosphoceramide (*N*-acetyl-GIPC).

MS^2-spectra were monitored in the negative ion mode for all molecular ions, and their fragmentation patterns were compared. The CID-$FTMS^2$-spectra of m/z 1273.7155 (3A), m/z 1287.7323 (3B), and m/z 1301.7457 (3C) are demonstrated in Figure 3. The fragment ions in MS^2-spectrum 3B were labeled according to the GIPC-nomenclature.[15,19] The nomenclature is clarified in Figure 4, by two different GIPC-structures. The polar head group in Figure 4A consists of hexose-hexuronic acid-inositol phosphate and in Figure 4B of *N*-acetylhexosamine-hexuronic acid-inositol phosphate. The only difference appeared in the terminal sugar moiety. Fragment ions derived from the *N*-acetylhexosamine-hexuronic acid-head group (Figure 4B) were labeled with an asterisk (*) and abbreviated in the following as *N*-acetyl-GIPC. GIPC-species with hexose as the terminal sugar moiety (Figure 4A) were named hexose-GIPC.

The MS^2-spectra shown in Figure 3 have comparable fragmentation patterns. The fragment ions m/z 399.0325−399.0327 and m/z 638.1324−638.1325 occurred in the three spectra with the same intensity. The fragment ions of m/z 639−1284 had the same pattern but different accurate masses. The fragment ions with the highest intensity were m/z 894.6050 (3A), m/z 908.6207(3B), and m/z 922.6361 (3C). These fragment ions had the same differences as the molecular ions $[M - H]^-$ in (3A) m/z 1273.7155, (3B) m/z 1287.7323, and (3C) m/z 1301.7457. Mass differences of 14.0154−14.0158 u were detected for all fragment ions with $m/z > 700$ in the MS^2-spectra shown in Figure 3. Fragment ions with $m/z < 700$ were identified as fragments of the polar head group. Ceramide-derived fragment ions were located in the mass range of m/z 639−1284 due to differences in the alkyl chain length. The fragmentation patterns were proven by comparing the detected accurate masses of the fragment ions with the calculated exact masses.

Comparison of PQD-$ITMS^2$- and CID-$FTMS^2$-Spectra in the Negative Ion Mode. The CID-$FTMS^2$-spectra were detected in a mass range of m/z 345 to 1315; for the analysis of smaller fragment ions PQD-$ITMS^2$-experiments were performed, which enabled the detection of fragment ions to $m/z > 50$. The PQD-$ITMS^2$-spectra of $[M - H]^-$ of m/z 1273.71 and m/z 1301.75 (see Figure S2 in the Supporting Information) presented a fragmentation pattern similar to that of the CID-$FTMS^2$-spectra (Figure 3A and 3C). Both fragmentation experiments generated the fragments $[C_3PO_3 - H]^-$ (= m/z 638) and $[Y_1 - H]^-$ as the most intense signals. The fragment ion with m/z 78.6−78.7 referred to $[PO_3]^-$ (calculated exact mass m/z 78.9591) and the fragment ion m/z 258.9−259.0 to an inositol phosphate fragment $[IP]^-$ ($C_6H_{12}O_9P$, calculated exact mass m/z 259.0224), and after water elimination, $[IP - H_2O]^-$ with m/z 240.8−240.9 (calculated exact mass m/z 241.0118) were identified using PQD-$ITMS^2$ (see Figure S2, Supporting Information). MS^2-experiments by Ejsing et al. with inositol phosphoceramides from *Saccharomyces cerevisiae* resulted also in $[IP]^-$ fragment ions.[13]

Due to the use of different mass spectrometers, deviations of the m/z values were obtained by CID-$FTMS^2$ and PQD-$ITMS^2$. Measurements by FTMS enabled high mass accuracy and high mass resolution. The ion trap experiments are indicated with one decimal due to unit resolution of the quadrupole instrument. Table 2 displays fragment ions of CID-$FTMS^2$- and PQD-$ITMS^2$-experiments of the GIPC-species of spinach with the molecular ions m/z 1273.7155 and m/z 1301.7457. The same fragment ions occurred at $m/z < 638$, and differences of 28.0310−28.0315 u were detected for fragment ions with $m/z >$ 639.

The plant samples of white cabbage, sunflower seeds, and soybeans were analyzed in the same manner as for the structural profiling of GIPC-species. The same *N*-acetyl-GIPC-species as in spinach were detected in tomato leaves, sunflower seeds, and soybeans. Exact masses, retention times, and MS^2-spectra were in accordance with the results for spinach.

Interestingly, the analysis of white cabbage resulted in the detection of other GIPC-species. MS^2-spectra in the negative mode of the molecular ions $[M - H]^-$ m/z 1232.6925 and m/z 1260.7239 are presented in Figure 5. These GIPC-species belonged to the hexose-type GIPC with hexose-hexuronic acid-

Table 2. Fragment Ions of *$[M - H]^-$ *m/z* 1273.7191 and *$[M - H]^-$ *m/z* 1301.7505 by CID-FTMS^2- and PQD-ITMS^2-Experiments (Figure 3 and Figure S2) in Spinach[a]

MS^2 neg	*$[M - H]^-$		*$[M - H]^-$
CID-FTMS	1273.7191		1301.7505
PQD-ITMS		deviation	
$[fragment\ ion]^-$	*m/z*	u	*m/z*
$[PO_3]^-$	*78.7*	*0.1*	*78.6*
$[IP - H_2O]^-$	*241.0*	*0.0*	*241.0*
$[IP]^-$	*259.0*	*0.0*	*259.0*
$[*C_3PO_3 - *C_1 - CO_2 - H]^-$	373.0533	0.00	373.0533
$[*C_3PO_3 - *C_1 - H_2O - H]^-$	399.0325	0.00	399.0325
$[*C_3PO_3 - *C_1 - H]^-$	417.0429	0.00	417.0431
$[*B_3 - H_2]^-$	540.1559	0.00	540.1559
$[*B_3PO_3 - H]^-$	620.1220	0.00	620.1221
$[*C_3PO_3 - H]^-$	638.1324	0.00	638.1324
	638.2		*638.2*
$[Z_0PO_3 - H]^-$	714.5427	28.0313	742.5740
$[Y_0PO_3 - H]^-$	732.5531	28.0315	760.5846
$[Y_1 - H]^-$	894.6051	28.0311	922.6362
	894.7		*922.7*
$[Y_1 + 42 - H]^-$	936.6161	28.0310	964.6471
$[Z_2 - CO_2 - H_2O - H]^-$	990.6266	28.0310	1018.6576
$[Z_2 - CO_2 - H]^-$	1008.6371	28.0313	1036.6684
$[Z_2 - H]^-$	1052.6266	28.0312	1080.6578
$[Y_2 - H]^-$	1070.6375	28.0311	1098.6686
$[M - H_2O - H]^-$	1255.7058	28.0314	1283.7372

[a]PQD-ITMS^2-fragment ions are indicated in italic font (for nomenclature of the fragment ions, see Figure 4).

inositol phosphate as polar head group, which were described by Markham et al. in *A. thaliana*.[10] The fragment ions had a fragmentation pattern similar to that for *N*-acetyl-GIPC; the most intense signal was represented by $[Y_1 - H]^-$, and the polar head group moiety led to the fragment ion $[C_3PO_3 - H]^-$ with *m/z* 597.1060. The same hexose-GIPC were identified in sunflower seeds and soybeans.

Analysis of the Fragmentation Pattern of Hexose- and N-Acetyl-GIPC in the Negative Ion Mode. To compare the differences in the fragmentation pattern of hexose- and *N*-acetyl-GIPC, the fragment ions of $[M - H]^-$ *m/z* 1260.7239 (white cabbage, Figure 5B) and of *$[M - H]^-$ *m/z* 1301.7505 (spinach, Figure 3C) are summarized in Table 3. As can be seen from Table 3, the MS^2-spectra of hexose- and *N*-acetyl-GIPC resulted in identical ceramide-fragment ions labeled with √ but in different *m/z* values for their polar head group containing fragment ions (e.g., $[C_3PO_3 - H]^-$) labeled with X.

Fragment ions containing the terminal sugar, as $[B_3 - H_2]^-$, $[B_3PO_3 - H]^-$, and $[C_3PO_3 - H]^-$, had a mass difference of 41.0266 u due to the exchange of a hydroxy group with a *N*-acetyl group. The cleavage of the terminal sugar C_1 resulted in identical fragment ions $[C_3PO_3{-}C_1 - H]^-$, as the remaining polar head group consisted of the same sugars.

The measured accurate masses of $[Y_0PO_3 - H]^-$ (phosphoceramide), $[Y_1 - H]^-$ (inositol phosphoceramide), and $[Y_2 - H]^-$ (hexuronic acid-inositol phosphoceramide) were identical. The difference of $[Y_2 - H]^-$ and $[Y_1 - H]^-$ with 176.0320−176.0324 correlated with the loss of hexuronic acid (calculated exact mass 176.0321 u) and the difference of $[Y_1 - H]^-$ and $[Y_0PO_3 - H]^-$ with 162.0516−162.0520 u to the cleavage of a hexose (inositol, exact mass 162.0528 u). The retention time of both GIPC-species was 10.9 min, and the different polar head group did not seem to affect the interaction of the analyte with the RP-Amide material.

GIPC in plants are known to contain the sphingoid bases t18:0 and t18:1 in high amounts and less of d18:0 or d18:1. Chain lengths of C16−26 of saturated, monohydroxylated fatty acids

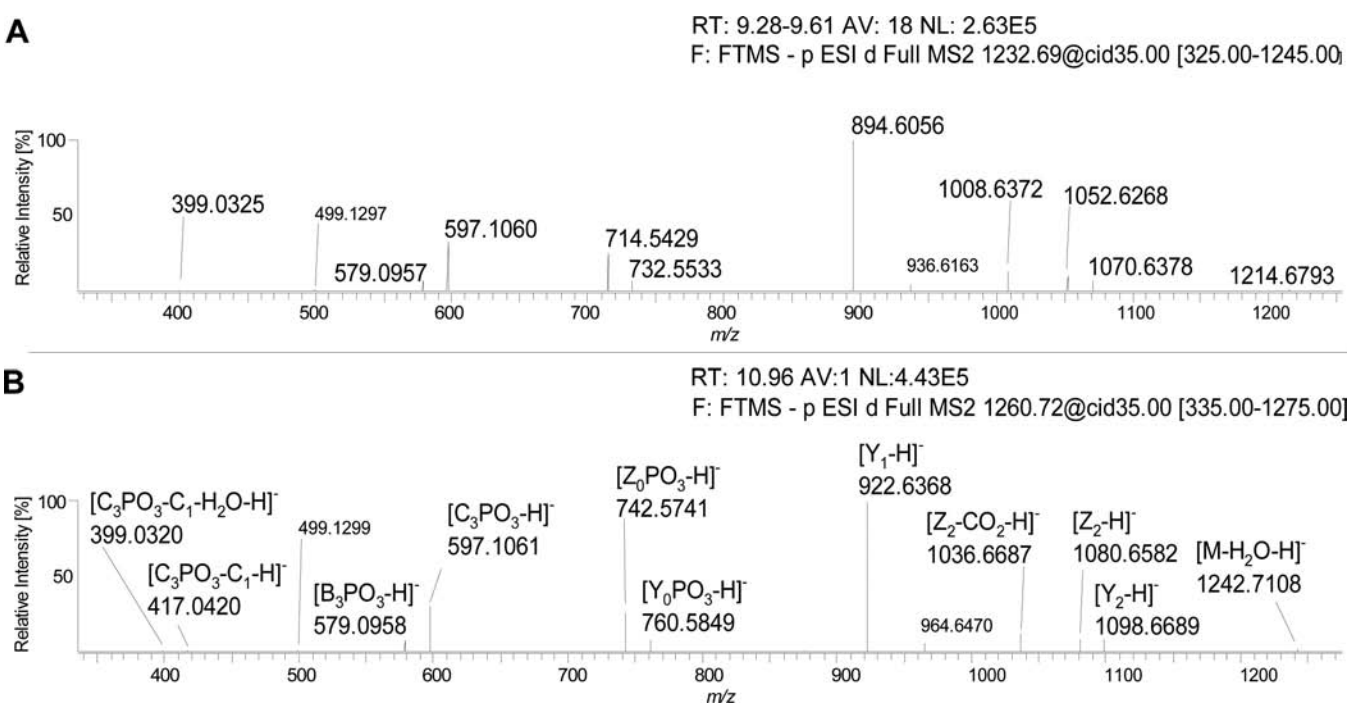

Figure 5. CID-FTMS^2-product ion spectra of $[M - H]^-$ *m/z* 1232.6925 (A) and *m/z* 1260.7239 (B) in white cabbage. GIPC nomenclature according to Figure 4 was applied in spectrum B. Fragment ions of *m/z* < 600 were identical and *m/z* > 600 had a difference of 28.0312−28.0315 u (HPLC-FTMS method 2).

dx.doi.org/10.1021/jf4001499 | J. Agric. Food Chem. 2013, 61, 4257−4269

Table 3. Fragment Ions of $[M - H]^-$ *m/z* 1260.7239 (White Cabbage, Figure 5B) and of $*[M - H]^-$ *m/z* 1301.7505 (Spinach, Figure 3C) by CID-FTMS^2- and PQD-ITMS^2-Experiments[a]

white cabbage				spinach
$[M - H]^-$		MS^2 neg		$*[M - H]^-$
1260.7239		CID-FTMS		1301.7505
ret time 10.6–11.5 min		*PQD-ITMS*		ret time 10.8–11.2 min
$[fragment\ ion]^-$	*m/z*		*m/z*	$[fragment\ ion]^-$
$[IP\text{-}H_2O]^-$	*241.0*	√	*241.0*	$[IP - H_2O]^-$
$[IP]^-$	*259.0*	√	*259.0*	$[IP]^-$
$[C_3PO_3 - C_1 - CO_2 - H]^-$	373.0531	√	373.0533	$[*C_3PO_3 - *C_1 - CO_2 - H]^-$
$[C_3PO_3 - C_1 - H_2O - H]^-$	399.0326	√	399.0325	$[*C_3PO_3 - *C_1 - H_2O - H]^-$
$[C_3PO3 - C_1 - H]^-$	417.0431	√	417.0431	$[*C_3PO_3 - *C_1 - H]^-$
$[C_3PO_3 - B_1 - H]^-$	435.0537		nd[b]	$[*C_3PO_3 - B_1 - H]^-$
$[B_3 - H_2]^-$	499.1298	X	540.1559	$[*B_3 - H_2]^-$
$[B_3PO_3 - H]^-$	579.0957	X	620.1221	$[*B_3PO_3 - H]^-$
$[C_3PO_3 - H]^-$	597.1060	X	638.1324	$[*C_3PO_3 - H]^-$
	597.3	X	*638.2*	
$[Z_0PO_3 - H]^-$	742.5740	√	742.5740	$[Z_0PO_3 - H]^-$
$[Y_0PO_3 - H]^-$	760.5846	√	760.5846	$[Y_0PO_3 - H]^-$
$[Y_1 - H]^-$	922.6366	√	922.6362	$[Y_1 - H]^-$
	922.7	√	*922.7*	
$[Y_1 + 42 - H]^-$	964.6470	√	964.6471	$[Y_1 + 42 + H]^-$
	nd		1018.6576	$[Z_2 - CO_2 - H_2O - H]^-$
$[Z_2 - CO_2 - H]^-$	1036.6686	√	1036.6684	$[Z_2 - CO_2 - H]^-$
$[Z_2 - H]^-$	1080.6579	√	1080.6578	$[Z_2 - H]^-$
$[Y_2 - H]^-$	1098.6686	√	1098.6686	$[Y_2 - H]^-$
$[M - H_2O - H]^-$	1242.7102	X	1283.7372	$*[M - H_2O - H]^-$

[a]Correlations of fragment ions were labeled with √ and differences of *m/z* values with X, and PQD-ITMS^2-fragment ions were indicated in italic font (for nomenclature of the fragment ions, see Figure 4). [b]nd = not detected.

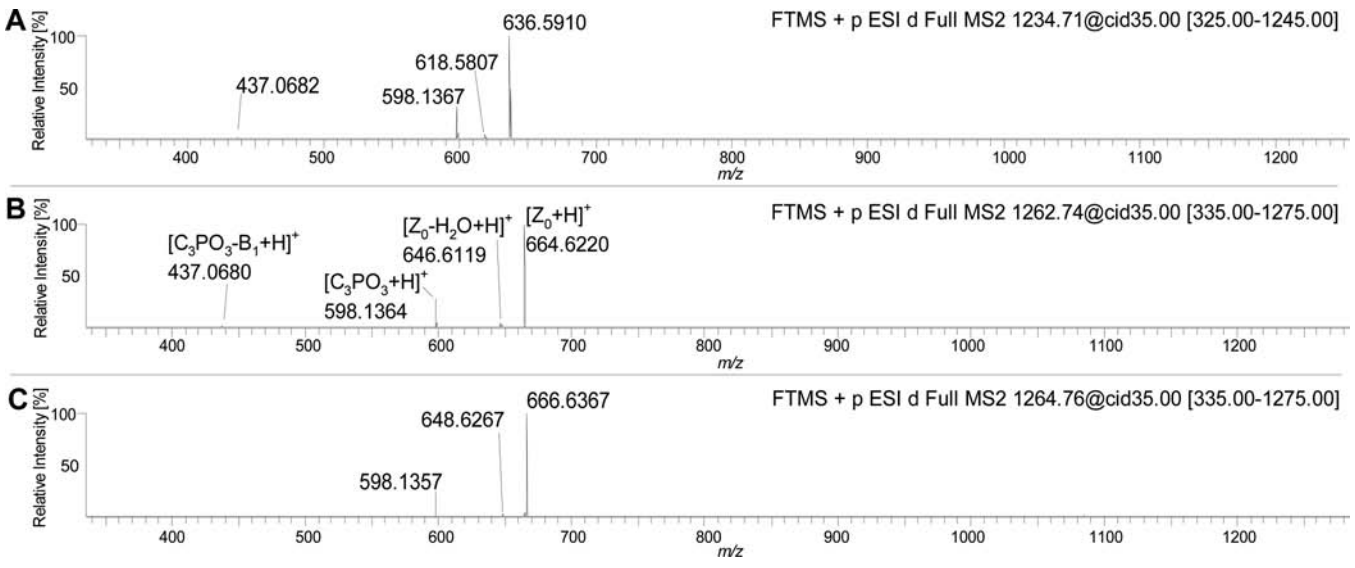

Figure 6. CID-FTMS^2-product ion spectra of $[M + H]^+$ *m/z* 1234.7082 (A), *m/z* 1262.7396 (B) and *m/z* 1264.7553 (C) in white cabbage. Fragment ions in spectrum B were labeled according to the nomenclature in Figure 4. The fragment ions $[Z_0 + H]^+$ arose with highest signal intensity and had the same deviations as their $[M + H]^+$, from A to B with 28.0314 u and B to C with 2.0157 u. All spectra contained $[C_3PO_3 + H]^+$ at *m/z* 598.1357–598.1367 (HPLC-FTMS method 1).

were identified.[11] GIPC with unsaturated fatty acids have not been reported.

Structure Elucidation by FTMS in the Positive Ion Mode To Characterize the Ceramide Moiety of GIPC. The GIPC-MS^2-spectra in the negative mode revealed neither fatty acid nor sphingoid base fragment ions. The ceramide-fragment ion of t18:1/h24:0 and t18:0/h24:1 would lead to the same exact mass. Therefore, MS^2-experiments in the positive mode were performed to characterize the ceramide-moiety of the GIPC.

In the following, GIPC of white cabbage with $[M + H]^+$ signals at *m/z* 1234.7082 (6A), *m/z* 1262.7396 (6B), and *m/z* 1264.7553 (6C) were analyzed by CID-FTMS^2 in the positive mode (Figure 6). On the basis of the exact mass, the most intense fragment ion $[Z_0 + H]^+$ was identified as the ceramide-fragment

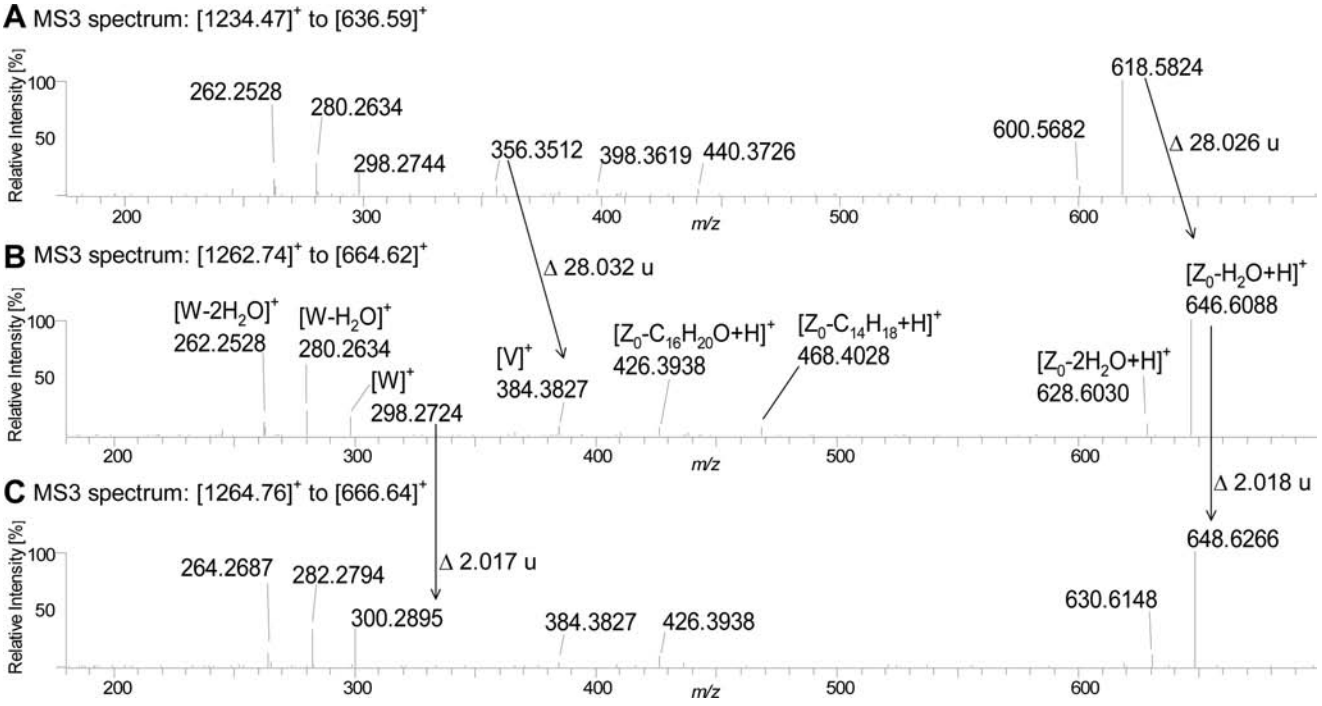

Figure 7. CID-FTMS^3-product ion spectra of $[M + H]^+$ to the corresponding ceramide fragment $[Z_0 + H]^+$ in sunflower seeds. Spectrum A belonged to m/z 1234.7082 and m/z 636.5910, spectrum B to m/z 1262.7396 and m/z 664.6220, and spectrum C to m/z 1264.7553 and m/z 666.6367. Nomenclature (Figure 4) was applied in MS^3-spectrum B. (HPLC-FTMS method 3).

ion. The mass differences of the molecular ions and their $[Z_0 + H]^+$ fragment ions were identical with 28.0314 u from 6A to 6B and 2.0157 u from 6B to 6C. The three MS^2-spetra contained the fragment ion m/z 598.1357−598.1367, which corresponded to the polar head group $[C_3PO_3 + H]^+$. The loss of the terminal hexose gave $[C_3PO_3 - B_1 + H]^+$ at m/z 437.0680−437.0682 as fragment ion.

The positive MS^2-spectra did not result in detailed structural information of the fatty acids and sphingoid bases in the ceramide part. As the $[Z_0 + H]^+$ fragment ion appeared in high intensity, it was chosen for further fragmentation experiments (FTMS^3). The molecular ion $[M + H]^+$ was fragmented, and in the next step the $[Z_0+H]^+$ fragment ion was selected and again fragmented. Figure 7 demonstrated the CID-FTMS^3-spectra of m/z 1234.7082 to m/z 636.5910 (7A), m/z 1262.7396 to m/z 664.6620 (7B), and m/z 1264.7553 to m/z 666.6367 (7C). The fragment ions were labeled according to the nomenclature of Costello and Levery.[15,19] Fragment ion $[V]^+$ consists of the fatty acid including the amino group, and $[W]^+$ contains the sphingoid base including the amino group.

The fragmentation pattern of $[Z_0 + H]^+$ showed the elimination of one and two molecules of water resulting in $[Z_0 - H_2O + H]^+$ and $[Z_0 - 2H_2O + H]^+$. Elimination of one and two water molecules was as well detected for the fragment ions m/z 298.2724−298.2744 (7A and 7B) and at m/z 300.2895 (7C).

The calculated exact mass of the sphingoid base fragment ion $[W]^+$ of t18:1 was m/z 298.2746, which was detected in spectra A and B shown in Figure 7. Spectrum C of Figure 7 displayed the fragment ion m/z 300.2895 (calculated exact mass m/z 300.2903) corresponding to the saturated sphingoid base t18:0. In the case of trihydroxy sphingoid bases the loss of two hydroxy groups was expected,[20] as can be seen for the sphingoid base fragment ions $[W]^+$ at m/z 298.2724−298.2744 (A and B) and at m/z 300.2895 (C) in Figure 7. In contrast, dihydroxy sphingoid bases with only one loss of water were not detectable. The fragment ion $[V]^+$ m/z 384.3827 arose in spectra 7B and 7C and was identified as monohydroxylated fatty acid fragment ion h24:0. The mass difference of $[M + H]^+$ m/z 1234.7082 (7A) and m/z 1262.7396 (7B) was the same as that of $[V]^+$ m/z 356.3512 (7A) and m/z 384.3827 (7B) with 28.0264−28.0315 u. In spectra 7B and 7C the fatty acid $[V]^+$ fragment ion m/z 384.3827 is identical, but the ceramide moiety contained different sphingoid bases. The molecular ions m/z 1234.7082 (7A) and m/z 1262.7396 (7B) had t18:1 as sphingoid base and m/z 1264.7553 (7C) t18:0.

The fatty acid linked to an amino group had a calculated exact mass of m/z 384.3842 ($C_{24}H_{50}NO_2$), the detected fragment ions in spectra 7B and 7C appeared with a mass deviation of 0.0015 u (4 ppm). The fragment ion m/z 356.3529 (7A) belonged to the fatty acid h22:0 linked to an amino group ($C_{22}H_{46}NO_2$).

MS^3-experiments were performed to characterize the ceramide moiety in detail. GIPC-species with a difference of 2.0178 u like that of the molecular ions $[M + H]^+$ m/z 1262.7396 and m/z 1264.7553 of spectra B and C in Figure 7 were analyzed to detect if the double bond was localized in the fatty acid or in the sphingoid base.

Structural Profiling of the Polar Head Group by FTMS in the Negative Ion Mode. Using a mass spectrometric approach, Markham et al. identified two GIPC polar head groups, in *A. thaliana* hexose-hexuronic acid-inositol phosphate and in tomato leaves *N*-acetylhexosamine-hexuronic acid-inositol phosphate.[10] Additional hexoses such as mannose and galactose, or pentoses such as arabinose, have been identified;[2,21] therefore, MS^2-spectra of GIPC-species were screened for those mass differences.

In the first experiments the polar head group fragment ions of $[C_3PO_3 - H]^-$ m/z 638.1324 (*N*-acetyl-GIPC) and m/z 597.1060 (hexose-GIPC) were analyzed by CID-FTMS^3-experiments in the negative mode. The molecular ion $[M - H]^-$ was

dx.doi.org/10.1021/jf4001499 | J. Agric. Food Chem. 2013, 61, 4257−4269

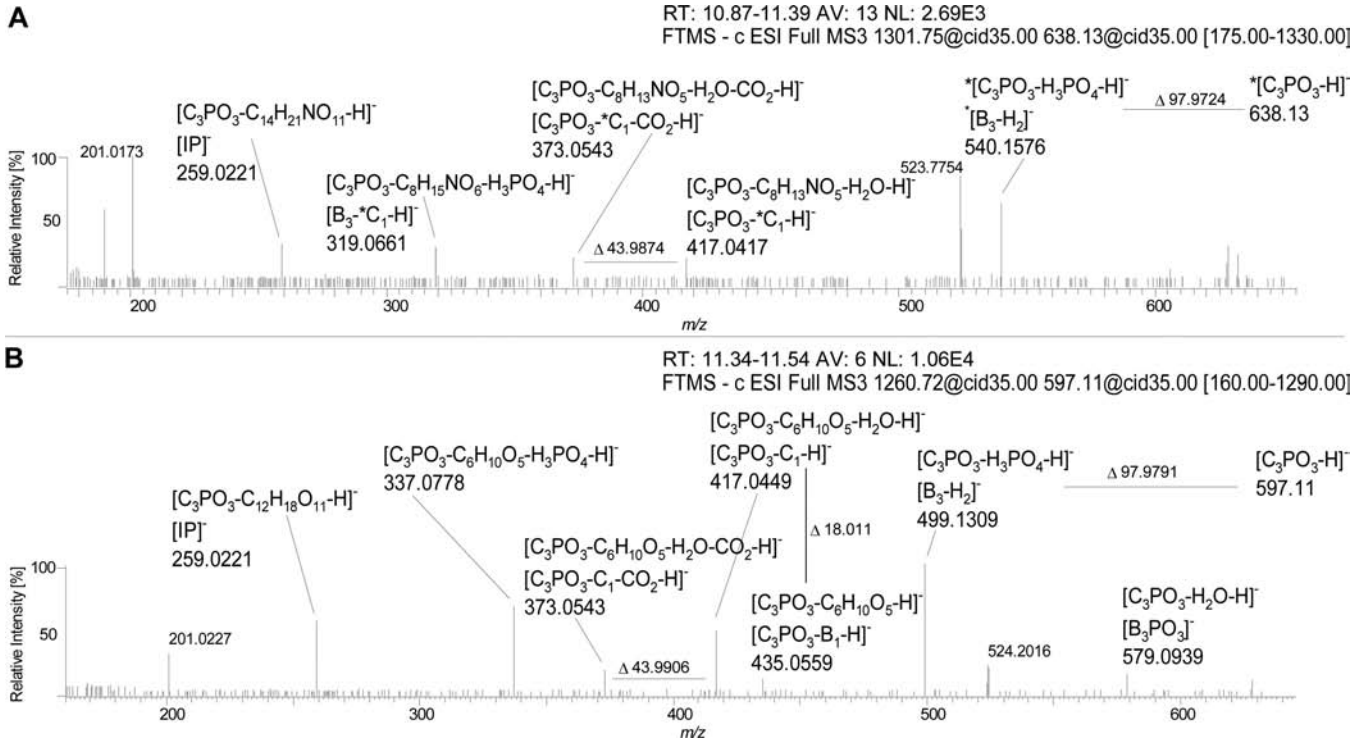

Figure 8. CID-FTMS^3-product ion spectra of $[M - H]^-$ to the polar head group fragment ion $[C_3PO_3 - H]^-$. In spinach m/z 1301.7505 to m/z 638.1324 (A) and in sunflower seeds m/z 1260.7239 to m/z 597.1060 (B) were analyzed. Characteristic fragment ions were labeled according to Figure 4 (HPLC-FTMS method 4).

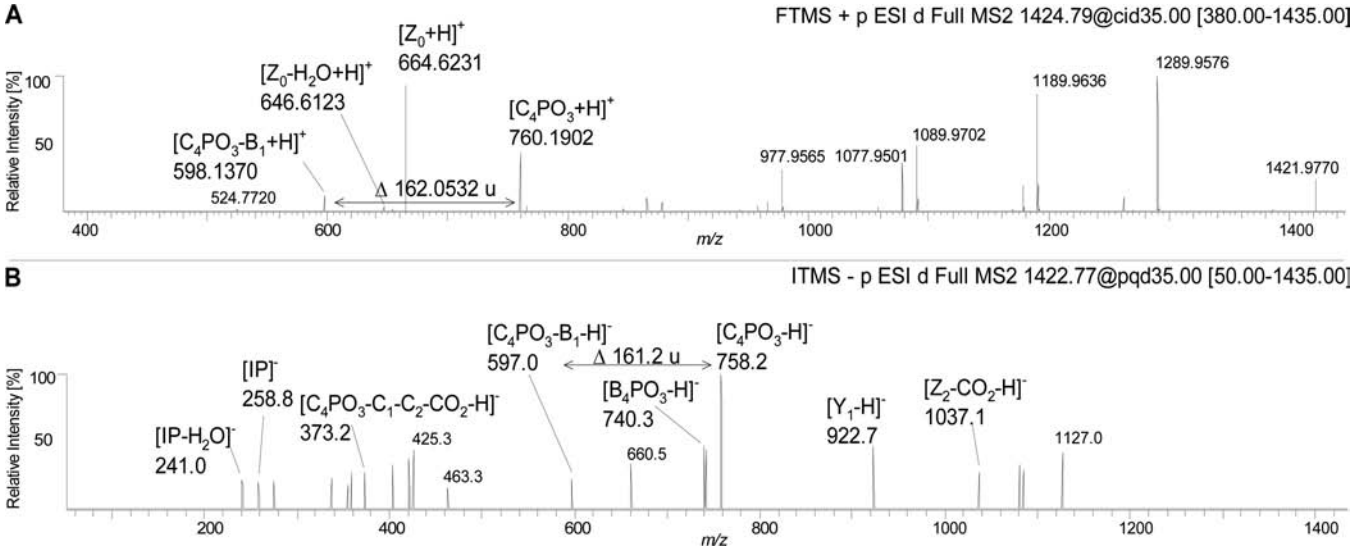

Figure 9. MS^2-product ion spectra of $[M + H]^+$ m/z 1424.7918 by CID-FTMS^2 (A) and of $[M - H]^-$ m/z 1422.7762 by PQD-ITMS^2 (B) of tomato leaves extract (HPLC-FTMS method 1 and 2).

fragmented, and the product ion $[C_3PO_3 - H]^-$ was selected for further fragmentation (Figure 8). The reported fragment ion $[IP]^-$ occurred in both MS^3-spectra, and the calculated exact mass was m/z 259.0224, which led to a deviation of 0.003 u (1 ppm). The loss of H_3PO_4 could be detected by the fragmentation of $[C_3PO_3 - H]^-$ to $[C_3PO_3 - H_3PO_4 - H]^-$ due to the mass difference of 97.9724−97.9791 u (calculated exact mass H_3PO_4 m/z 97.9769).

The elimination of the terminal sugar residue resulted in the fragment ions m/z 417.0417 and m/z 373.0543. The difference of $*[C_3PO_3 - H]^-$ with m/z 638.1324 to $[C_3PO_3 - *C_1 - H]^-$ with m/z 417.0417 was 221.0907 u for the spectrum shown in Figure 8A and 180.0611 u in spectrum 8B. These mass differences, assigned as C_1 according to Figure 4, corresponded to *N*-acetylhexosamine in spectrum 8A with the calculated exact mass of m/z 221.0899 and to a hexose in spectrum 8B with a calculated exact mass of m/z 180.0634. The fragment ion m/z 373.0543 occurred in both spectra due to the loss of the terminal sugar and a carboxyl group. The detected difference of $[C_3PO_3 - C_1 - H]^-$ to $[C_3PO_3 - C_1 - CO_2 - H]^-$ was 43.9874 u and matched very well with the calculated exact mass of CO_2 with m/z 43.9898. The decarboxylation may take place at the hexuronic

dx.doi.org/10.1021/jf4001499 | J. Agric. Food Chem. 2013, 61, 4257−4269

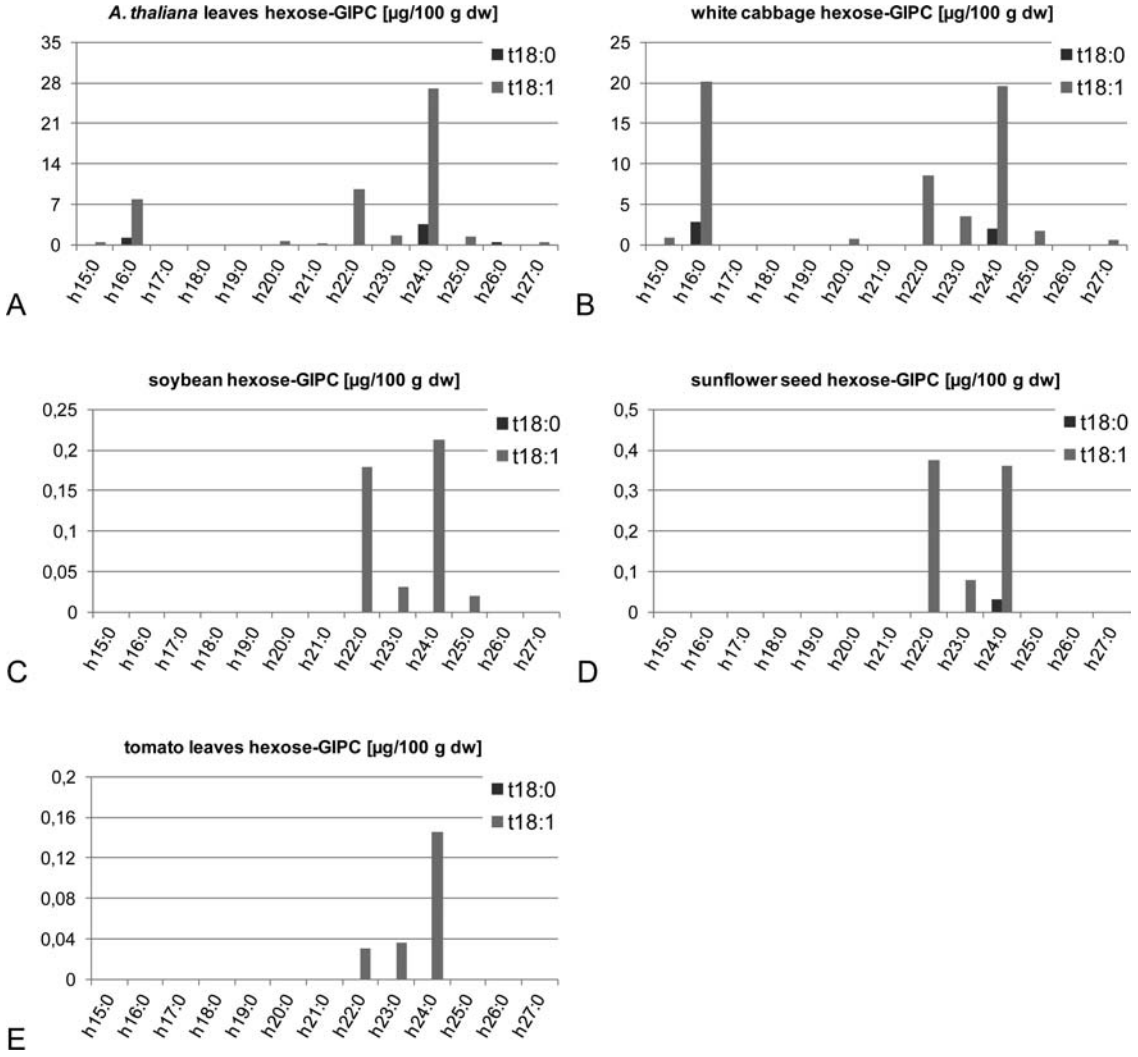

Figure 10. Hexose-GIPC amounts (µg/100 g dw) in *A. thaliana* (A), white cabbage (B), soybeans (C), sunflower seeds (D), and tomato leaves (E). Monohydroxylated fatty acids are designated by the numbers of carbon atoms (h15:0–h27:0) which are linked to the sphingoid bases t18:0 and t18:1 (n = 2, mean).

acid moiety. The fragment ions in MS^3-spectra 8A and 8B with a difference of 41.0264–41.0267 u were proof that the terminal sugar was still a part of the fragment ion as in $[B_3 - H_2]^-$ with m/z 540.1576 (8A) and m/z 499.1309 (8B) or $[C_3PO_3 - H]^-$ with m/z 638.1324 (8A) and m/z 597.1060 (8B). The loss of H_3PO_4 (97.9756 u) was detected from $[{}^*C_3PO_3 - {}^*C_1 - H]^-$ with m/z 417.0417 to $[B_3 - {}^*C_1 - H]^-$ with m/z 319.0061 in spectrum 8B (Figure 8). The resulting fragment ion $[B_3 - {}^*C_1 - H]^-$ consisted of inositol and hexuronic acid, and the negative charge can be stabilized by the carboxylic group.

Detection of GIPC with Hexose-Hexose-Hexuronic Acid-Inositol Phosphate as Polar Head Group. The analysis of molecular ions of m/z > 1400 in tomato leaves led to known hexose-GIPC fragment ions for the ceramide and polar head group moiety. In Figure 9 the CID-$FTMS^2$-spectrum in the positive ion mode of m/z 1424.7918 (9A) and the PQD-$ITMS^2$-spectrum in the negative ion mode of m/z 1422.7762 (9B) are illustrated. The ceramide fragment ion $[Z_0 + H]^+$ of m/z 664.6231 was already detected in the CID-$FTMS^2$ of $[M + H]^+$ with m/z 1262.7396 in Figure 6B. The polar head group fragment ion for hexose-hexuronic acid-inositol phosphate with m/z 598.1370 arose as well in spectrum 9A. The fragment ion m/z 760.1902 in spectrum 9A occurred with a mass difference of 162.0532 u to m/z 598.1370. The calculated exact mass of a hexose with one loss of water ($C_6H_{10}O_5$) was 162.0528 u with a mass deviation of 0.0004 u (2 ppm). $FTMS^2$-experiments in the negative ion mode were not successful because of low signal intensities for this analyte. Instead PQD-$ITMS^2$-experiments were performed (spectrum 9B). Known fragment ions such as $[IP]^-$, $[IP - H_2O]^-$, and the polar head group fragment ion m/z 597.0 were detected. The suggestion, that the polar head group contains an additional hexose was verified, as the fragment ion m/z 758.2 was 161.2 u heavier than m/z 597.0. The ceramide fragment ion $[Y_1 - H]^-$ with m/z 922.7 was, as well, detected in MS^2-experiments of m/z 1260.7239 (Figure 9B).

These fragmentation experiments confirmed the occurrence of GIPC-species with the polar head group consisting of hexose-hexose-hexuronic acid-inositol phosphate. Characterization of the ceramide by the MS^2-spectrum was not successful because of low signal intensities. The exact mass of the ceramide fragment ion $[Z_0 + H]^+$ of m/z 664.6231 could be originated by t18:1/h24:0 or t18:0/h24:1. GIPC-species with four sugars were identified in tomato leaves, and their occurrence in other plant samples could not be confirmed by mass spectrometric investigations. It was assumed that GIPC with longer oligosaccharide chains are ubiquitous in plant sources. In-source

dx.doi.org/10.1021/jf4001499 | J. Agric. Food Chem. 2013, 61, 4257–4269

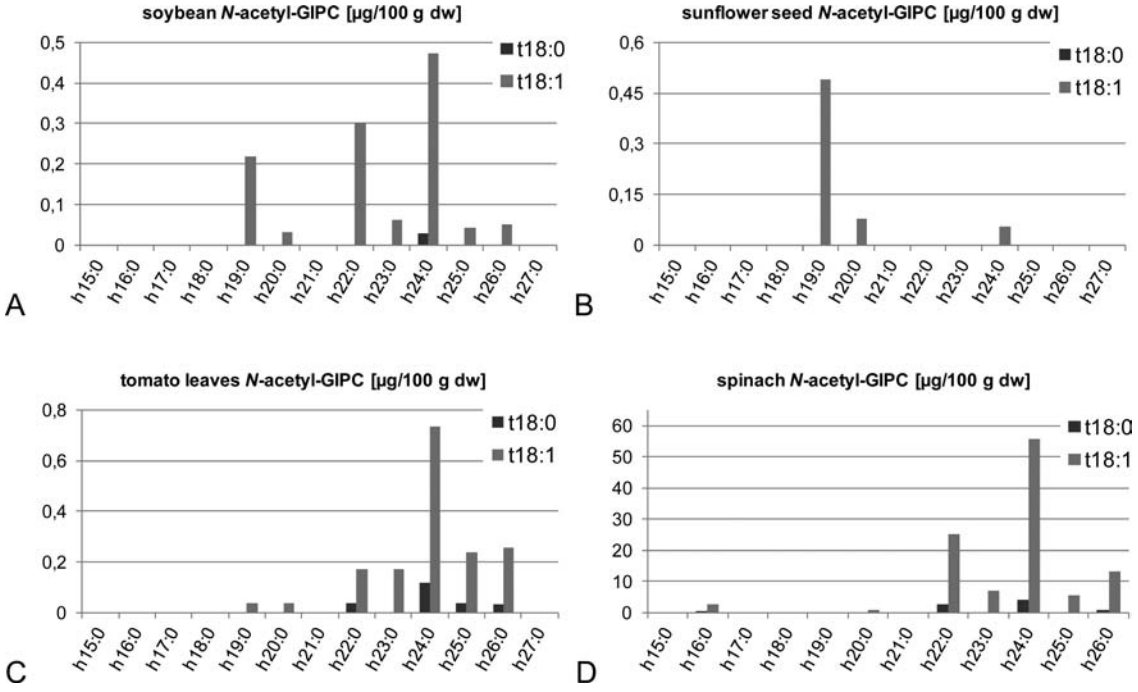

Figure 11. *N*-Acetyl-GIPC amounts (μg/100 g dw) in soybeans (A), sunflower seeds (B), tomato leaves (C), and spinach (D). Monohydroxylated fatty acids are designated by the numbers of carbon atoms (h16:0−h26:0) which are linked to the sphingoid bases t18:0 and t18:1 (n = 2, mean).

fragmentation of unstable GIPC may cause the low signal intensities. Soft ionization by MALDI-MS/MS enabled the detection of GIPC with polar head groups of two to seven sugars in tobacco leaves.[14]

Quantitation of GIPC in Plant Material. For the quantitation of GIPC in plant material, sphingosyl phosphoinositol (lyso-IPC) was used as quantitation standard in the calibration curve. Lyso-IPC has structural similarities to GIPC, e.g., the sphingoid base and the inositol phosphate group, and is a useful quantitation standard, as no GIPC standards are available. In addition, all samples including calibration curve standards and plant extracts were spiked with C17-inositol phosphoceramide (C17-IPC) to compensate for matrix effects due to coeluting matrix compounds, which might influence the ionization efficiency. The quantitation was performed by HPLC-FTMS in the negative ion mode (method 2). GIPC with monohydroxylated, saturated fatty acids h15−27 and with the trihydroxy sphingoid bases t18:0 and t18:1 were analyzed. Two GIPC-species with different polar head groups were quantified in leaves of *A. thaliana*, tomato, spinach, white cabbage, sunflower seeds, and soybeans. The oligosaccharide chains consisted of *N*-acetylhexosamine-hexuronic acid-inositol (*N*-acetyl-GIPC) and of hexose-hexuronic acid-inositol (hexose-GIPC).

The following GIPC-amounts are semiquantitative, as the internal standards did not have the same physical and chemical properties as the GIPC-species. A recovery rate could not be determined because of low amounts of lyso-IPC and C17-IPC. The GIPC-amounts were corrected regarding the purity of the internal standard lyso-IPC (74% HPLC-ELSD). However, the observed results give a good overview for the occurrence of GIPC and their structural variety in different plant species. The structure of analyzed GIPC was proven by the exact mass of the molecular ions $[M - H]^-$, $ITMS^2$-, and $FTMS^2$-fragment ion spectra and by the retention time. The amounts of *N*-acetyl-GIPC and hexose-GIPC in different plant species are summarized in Figures 10 and 11. Interestingly, the occurrence of both types of GIPC with hexose-hexuronic acid-inositol phosphate and *N*-acetylhexosamine-hexuronic acid-inositol phosphate as head group were not homogeneously distributed in the different plant sources. In the samples of *A. thaliana* and white cabbage, only hexose-GIPC were identified; spinach contained *N*-acetyl-GIPC, and soybeans, sunflower seeds, and tomato leaves comprised both types of GIPC.

The main ceramide structure in both GIPC-classes was the combination t18:1/h24:0, as first reported by Markham et al.[10,12,14] The lowest amount of hexose-GIPC with t18:1/h24:0 was 0.15 μg/100 g dry weight (dw) in tomato leaves, and the highest was 27.13 μg/100 g dw in *A. thaliana* (Figure 10). The lowest amount of *N*-acetyl-GIPC with t18:1/h24:0 was 0.06 μg/100 g dw in sunflower seeds, and the highest was 55.67 μg/100 g dw in spinach (Figure 11). Ceramides with fatty acids of carbon chain length of >C22 showed increased amounts compared to ceramides with shorter fatty acids, such as the C16 fatty acid. A middle chain fatty acid such as h16:0 was identified in *A. thaliana*, white cabbage, and spinach (Figure 10). The amount of even-numbered fatty acids exceeded that of odd-numbered fatty acids. This is the first report of GIPC with odd-numbered fatty acids such as h19:0 in *N*-acetyl-GIPC and h23:0 in hexose-GIPC. In both GIPC-classes, t18:1 appeared in higher amounts than saturated t18:0.

The total GIPC-content of hexose-GIPC and *N*-acetyl-GIPC in *A. thaliana*, white cabbage, and spinach ranged from 40.5 to 88.4 μg/100 g dw and in soybean, sunflower seed, and tomato leaves from 1.1 to 1.6 μg/100 g dw (see Figure S3 in the Supporting Information).

We successfully developed a $HPLC\text{-}FTMS^n$ method for structural profiling of GIPC in various plant materials. MS^2-experiments in the negative and positive mode of GIPC resulted in specific fragment ions, originating from their polar head groups. MS^3-fragmentation provided important structural information for the ceramide backbone. By comparing the MS^2- and MS^3-spectra acquired from hexose-GIPC and *N*-acetyl-

dx.doi.org/10.1021/jf4001499 | J. Agric. Food Chem. 2013, 61, 4257−4269

GIPC with different ceramide backbones, we demonstrated that GIPC yielded a common pattern of major fragment ions. Their structural assignment was achieved by the high mass accuracy of FTMS-experiments.

■ ASSOCIATED CONTENT

Supporting Information

Figure S1 demonstrates HPLC-FTMS chromatograms of the extracted accurate masses of $[M - H]^-$ m/z 1273.7155 (A), m/z 1287.7323 (B), and m/z 1301.7457 (C). PQD-ITMS^2-product ion spectra of $[M - H]^-$ m/z 1273.7155 (A) and m/z 1301.7457 (B) are presented in Figure S2. Total GIPC-content of hexose- and *N*-acetyl-GIPC in various plants is shown in Figure S3. This material is available free of charge via the Internet at http://pubs.acs.org

■ AUTHOR INFORMATION

Corresponding Author

*Tel: +49 251 8333391. Fax: +49 251 8333396. E-mail: humpf@wwu.de.

Funding

This project was funded by the Deutsche Forschungsgemeinschaft, Bonn (International Research Training Group Münster-Nagoya, GRK 1143).

Notes

The authors declare no competing financial interest.

■ ACKNOWLEDGMENTS

We thank Prof. Marcos Sergio de Toledo (Universidade Federal de São Paulo, Biochemistry Department, Brazil) for accepting Nina Blaas as an exchange student and for sharing his knowledge about GIPC. Prof. Norberto Peporine Lopes (Universidade de São Paulo, Faculdade de Ciências Farmacêuticas de Ribeirão Preto, Brazil) is sincerely thanked for the discussions about mass spectrometric analysis and for his support in Ribeirão Preto. We thank Prof. J. Kudla (University of Münster) for providing *A. thaliana* seeds and for offering a place for the cultivation. The magnetic macroporous cellulose beads were kindly provided by Dr. J. Lenfeld (Institute of Macromolecular Chemistry, Academy of Sciences of the Czech Republic, Prague, Czech Republic).

■ REFERENCES

(1) Imai, H.; Morimoto, Y.; Tamura, K. Sphingoid base composition of monoglucosylceramide in Brassicacae. *J. Plant Physiol.* **2000**, *157*, 453–456.

(2) Carter, H. E.; Strobach, D. R.; Hawthorne, J. N. Biochemistry of the sphingolipids. XVIII. Complete structure of tetrasaccharide phytoglycolipid. *Biochemistry* **1969**, *8*, 383–388.

(3) Worrall, D.; Ng, C. K.; Hetherington, A. M. Sphingolipids, new players in plant signaling. *Trends Plant. Sci.* **2003**, *8* (7), 317–320.

(4) Lynch, D. V.; Dunn, T. M. An introduction to plant sphingolipids and a review of recent advances in understanding their metabolism and function. *New Phytol.* **2004**, *161*, 677–702.

(5) Warnecke, D.; Heinz, E. Recently discovered functions of glucosylceramides in plants and fungi. *Cell. Mol. Life Sci.* **2003**, *60* (5), 919–941.

(6) Oxley, D.; Bacic, A. Structure of the glycosylphosphatidylinositol anchor of an arabinogalactan protein from *Pyrus communis* suspension-cultured cells. *Proc. Natl. Acad. Sci. U.S.A.* **1999**, *96* (25), 14246–14251.

(7) Thompson, G. A., Jr.; Okuyama, H. Lipid-linked proteins of plants. *Prog. Lipid Res.* **2000**, *39* (1), 19–39.

(8) Merrill, A. H., Jr.; Wang, M. D.; Park, M.; Sullards, M. C. (Glyco)sphingolipidology: an amazing challenge and opportunity for systems biology. *Trends Biochem. Sci.* **2007**, *32*, 457–468.

(9) Sperling, P.; Franke, S.; Luthje, S.; Heinz, E. Are glucocerebrosides the predominant sphingolipids in plant plasma membranes? *Plant. Physiol. Biochem.* **2005**, *43* (12), 1031–1038.

(10) Markham, J. E.; Li, J.; Cahoon, E. B.; Jaworski, J. G. Separation and identification of major plant sphingolipid classes from leaves. *J. Biol. Chem.* **2006**, *281* (32), 22684–22694.

(11) Markham, J. E.; Jaworski, J. G. Rapid measurement of sphingolipids from *Arabidopsis thaliana* by reversed-phase high-performance liquid chromatography coupled to electrospray ionization tandem mass spectrometry. *Rapid Commun. Mass Spectrom.* **2007**, *21* (7), 1304–1314.

(12) Salas, J. J.; Markham, J. E.; Martinez-Force, E.; Garces, R. Characterization of sphingolipids from sunflower seeds with altered fatty acid composition. *J. Agric. Food Chem.* **2011**, *59* (23), 12486–12492.

(13) Ejsing, C. S.; Moehring, T.; Bahr, U.; Duchoslav, E.; Karas, M.; Simons, K.; Shevchenko, A. Collision-induced dissociation pathways of yeast sphingolipids and their molecular profiling in total lipid extracts: a study by quadrupole TOF and linear ion trap-orbitrap mass spectrometry. *J. Mass Spectrom* **2006**, *41* (3), 372–389.

(14) Buré, C.; Cacas, J.-L.; Wang, F.; Gaudin, K.; Domergue, F.; Mongrand, S.; Schmitter, J.-M. Fast screening of highly glycosylated plant sphingolipids by tandem mass spectrometry. *Rapid Commun. Mass Spectrom.* **2011**, *25*, 3131–3145.

(15) Levery, S. B.; Toledo, M. S.; Straus, A. H.; Takahashi, H. K. Comparative analysis of glycosylinositol phosphorylceramides from fungi by electrospray tandem mass spectrometry with low-energy collision-induced dissociation of Li(+) adduct ions. *Rapid Commun. Mass Spectrom.* **2001**, *15* (23), 2240–2258.

(16) Merrill, A. H., Jr.; Sullards, M. C.; Allegood, J. C.; Kelly, S.; Wang, E. Sphingolipidomics: high-throughput, structure-specific, and quantitative analysis of sphingolipids by liquid chromatography tandem mass spectrometry. *Methods* **2005**, *36* (2), 207–224.

(17) Kuchar, L.; Rotkova, J.; Asfaw, B.; Lenfeld, J.; Horak, D.; Korecka, L.; Bilkova, Z.; Ledvinova, J. Semisynthesis of C17:0 isoforms of sulphatide and glucosylceramide using immobilised sphingolipid ceramide *N*-deacylase for application in analytical mass spectrometry. *Rapid Commun. Mass Spectrom.* **2010**, *24* (16), 2393–2399.

(18) Smith, S. W.; Lester, R. L. Inositol phosphorylceramide, a novel substance and the chief member of a major group of yeast sphingolipids containing a single inositol phosphate. *J. Biol. Chem.* **1974**, *249* (11), 3395–3405.

(19) Costello, C. E.; Vath, J. E. Tandem mass spectrometry of glycolipids. *Methods Enzymol.* **1990**, *193*, 738–768.

(20) Sugawara, T.; Aida, K.; Duan, J.; Hirata, T. Analysis of glucosylceramides from various sources by liquid chromatography-ion trap mass spectrometry. *J. Oleo Sci.* **2010**, *59* (7), 387–394.

(21) Kaul, K.; Lester, R. L. Isolation of six novel phosphoinositol-containing sphingolipids from tobacco leaves. *Biochemistry* **1978**, *17* (17), 3569–3575.